

## Finite element modelling of FRP-strengthened RC beam-column connections with ANSYS

Rijun Shrestha<sup>1</sup>, Scott T. Smith\*<sup>2</sup> and Bijan Samali<sup>1</sup>

<sup>1</sup>School of Civil and Environmental Engineering, University of Technology Sydney, NSW, Australia

<sup>2</sup>School of Environment, Science and Engineering, Southern Cross University, Lismore  
NSW 2480, Australia

(Received February 19, 2010, Revised March 2, 2011, Accepted November 29, 2011)

**Abstract.** There is an abundance of research on the strengthening of reinforced concrete (RC) structural elements such as beams, columns and slabs with fibre reinforced polymer (FRP) composites. Less research by comparison has been conducted on the strengthening of RC beam-column connections and the majority of such research has been predominantly experimental to date. Few existing experimental studies have reported extensive instrumentation of test specimens which in turn makes understanding the behavior of the connections and especially the contributions made by the FRP difficult to ascertain. In addition, there has been even more limited research on the analytical and numerical modelling of FRP-strengthened connections. In this paper, detailed descriptions of key strategies to model FRP-strengthened RC connections with finite elements are provided. An extensively instrumented and comprehensively documented set of experiments on FRP-strengthened connections is firstly presented and finite element models are then constructed using ANSYS. The study shows that the finite element approach is able to capture the overall behavior of the test specimens including the failure mode as well as the behavior of the FRP which will most importantly lead to a detailed understanding of the FRP and the future development of rational analytical models. The finite element models are, however, unable to model the stiffness of the connections with accuracy in the ultimate load range of response.

**Keywords:** concrete; connections; fibre reinforced polymers; finite elements; joints; strengthening

---

### 1. Introduction

The retrofitting/repair/strengthening (herein strengthening) of reinforced concrete (RC) structural elements such as beams, columns and slabs with externally bonded fibre-reinforced polymer (FRP) composites has been extensively studied over at least the last decade and comprehensive reviews are available in the open literature (e.g. Teng *et al.* 2003, ACI 440R-07 2007, Hollaway and Teng 2008). Surprisingly, very little research by comparison has been conducted on the strengthening of RC beam-column connections (also known as RC beam-column joints but herein referred to as connections) with FRP composites. The need to strengthen and/or enhance the ductility of connections stems from gravity load designed frames, designed prior to the need to consider seismic actions, being inherently weak within the connection region when

---

\*Corresponding author, Professor, E-mail: [Scott.Smith@scu.edu.au](mailto:Scott.Smith@scu.edu.au)

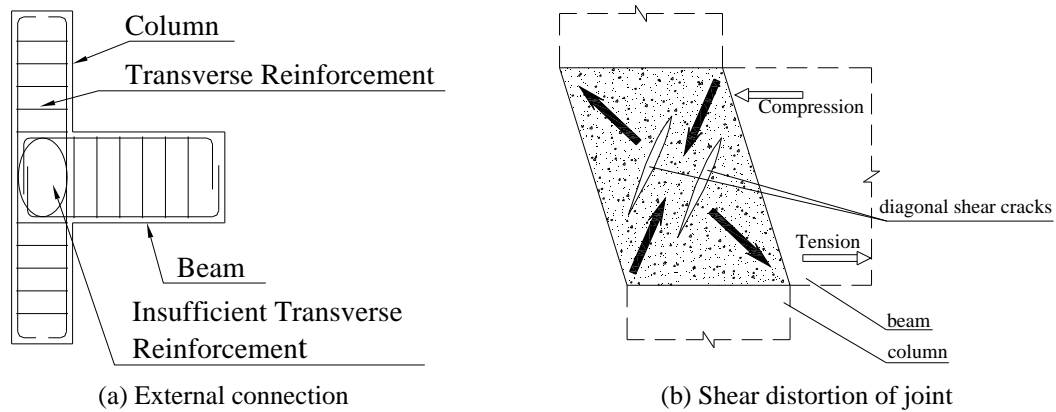


Fig. 1 Connections deficient in shear capacity

subjected to seismic attack. Common deficiencies are (1) poor joint shear strength due to lack of transverse reinforcement in the joint region (e.g. Fig. 1), (2) unanchored bottom longitudinal reinforcing bars may pull-out in the advent of load reversal from seismic attack, and (3) plastic hinge forming too close to the joint region in the beam (or column).

The majority of research that has been conducted on FRP-strengthened connections has been experimental. Both external and internal two-dimensional connections have been tested with externally bonded FRP in order to enhance the connection shear capacity (e.g. Antonopoulos and Triantafillou 2003, Shrestha *et al.* 2009, 2011), or to enhance the anchorage capacity of the longitudinal beam reinforcement (e.g. Granata and Parvin 2001). In addition, FRP has been used to enhance both the shear strength of the connection and anchorage of the beam reinforcement (e.g. El-Amoury and Ghobarah 2002) or relocate the formation of plastic hinging further along the beam away from the face of the connection (e.g. Mahini and Ronagh 2011a). In most test scenarios, both ends of the connection were typically secured and a load was applied to the free end of the beam (herein referred to as the *beam-tip*). A review of experimental research on the strengthening of RC connections with FRP in addition to an evaluation of the effectiveness of the tested strengthening schemes is given by Smith and Shrestha (2006). A review of non-FRP strengthening solutions, as well as some FRP ones, is given in Engindeniz *et al.* (2005).

As opposed to experimental testing, significantly less research has been undertaken on the numerical modelling of FRP-strengthened connections with non-linear finite element (FE) modelling being conducted by only a few researchers (Parvin and Granata 2000, Parvin and Wu 2004, Mostofinejad and Taleitaba 2006, Mahini and Ronagh 2011b). Parvin and Granata (2000) and Mostofinejad and Taleitaba (2006) developed three-dimensional non-linear FE models using ANSYS to model the behaviour of Granata and Parvin's (2001) test connections. These monotonically loaded tests were aimed at improving the anchorage of the top tension internal steel reinforcing beam bars in the connection region, by strengthening the top of the beam adjacent to the connection in flexure. The strengthened connection ultimately failed by breakdown of the anchorage used to secure the flexural strengthening on the beam. Parvin and Granata's (2000) study compared the failure loads to the FE model, in addition to reporting stress distributions in the FRP strengthening as well as the results of a parametric study. Mostofinejad and Taleitaba (2006), unlike Parvin and Granata (2000), considered slip between the steel reinforcing bars and surrounding concrete as well as the FRP and adjacent concrete substrate. Mostofinejad and

Talaeitaba (2006) generated the complete moment versus rotation relationship up to failure only for the FRP-strengthened connection which was found to correlate reasonably well with one of Granata and Parvin's (2001) tests. The ultimate moment and rotation were, however, over-predicted by approximately 20%. Parvin and Wu (2004) reported the results of parametric studies on FRP-strengthened connections, undertaken using the FE package MARC-MENTAT, but no comparisons were made with test results.

Manhini and Ronagh (2011b) developed three-dimensional non-linear FE ANSYS models and compared the predictions with the failure envelopes of cyclically loaded connections that had been strengthened with FRP on the sides of the connection and in the adjacent beam. The strengthening intended to relocate plastic hinging further along the beam away from the connection. They predicted the ultimate load of the plain connection well. The three reviewed studies which utilised ANSYS (i.e., Parvin and Granata 2000, Mostofinejad and Talaeitaba 2006, Mahini and Ronagh 2011b) used the concrete element which was capable of simulating concrete plastic deformation, crushing and cracking. To the best of the authors' knowledge, no researchers to date have numerically modelled shear-strengthened connections.

Overall, FE modelling of FRP-strengthened RC beam-column connections is a challenging prospect given the complexity of the connection geometry and stress concentrations at corners thus causing instabilities in the model. A need therefore exists to systematically address the relevant issues required to successfully model such connections and this paper addresses such a need. In this paper, the use of ANSYS (Version 11.0) to model the FRP shear-strengthened connection experiments reported in Shrestha (2009) and Shrestha *et al.* (2009) is reported in detail. Unlike the majority of tests reported to date, Shrestha's (2009) tests applied a monotonic load to the connection thus making the behaviour of the FRP strengthening and the joint region beneath to be accurately monitored. The complex cracking state inherent in cyclically loaded connections was removed and hence the clarity of the results was enhanced. In addition, Shrestha's (2009) experiments were extensively instrumented and documented thus further increasing the reliability and confidence of the test data. Following a description of the tests, a detailed background to the FE modelling techniques using ANSYS to model FRP-strengthened beam-column connections is then provided and the FE predictions are compared with the test data. Non-linearity is introduced into the models via the material constitutive relationships while certain simplifications are introduced (e.g. perfect bond between the FRP and concrete) in order to simplify the analysis. The effect of such simplifications is also discussed. Novel modelling techniques are also employed in order to avoid non-convergence of the model such as the use of a dummy element mesh. The ability of the FE model to accurately model the progression of cracking in the joint region, the failure mode of the joint and FRP, and the strain distribution along the FRP strengthening is demonstrated. Unfortunately the displacement was not captured well by the FE models and several reasons for this limitation are provided.

## 2. Experimental details

Three monotonically loaded connections are utilised in this study of which one was an unstrengthened control test (Specimen UM1) and two were strengthened with FRP strips (Specimens SM1 and SM2). FRP strips were chosen as opposed to sheets in order to monitor the progression of cracking in the joint region more easily in addition to detecting the occurrence of debonding of the FRP. A detailed account of the test specimens can be found in Shrestha (2009).

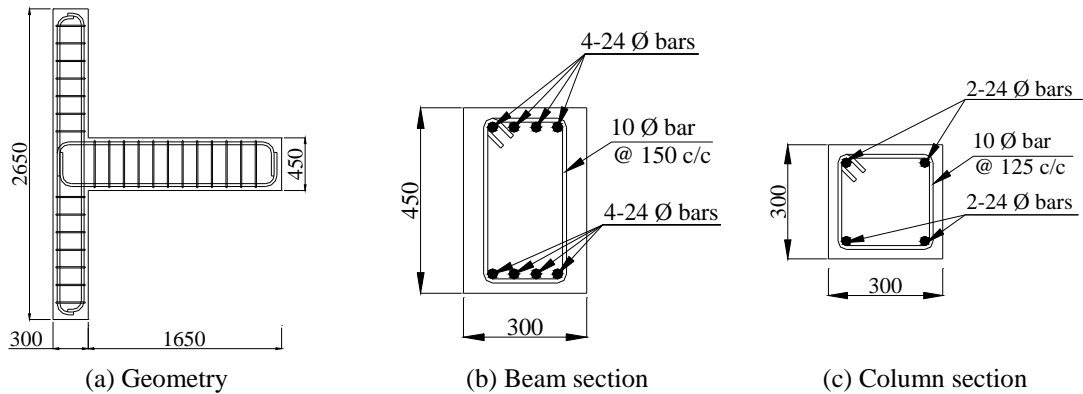


Fig. 2 Test connection – geometry and reinforcement details

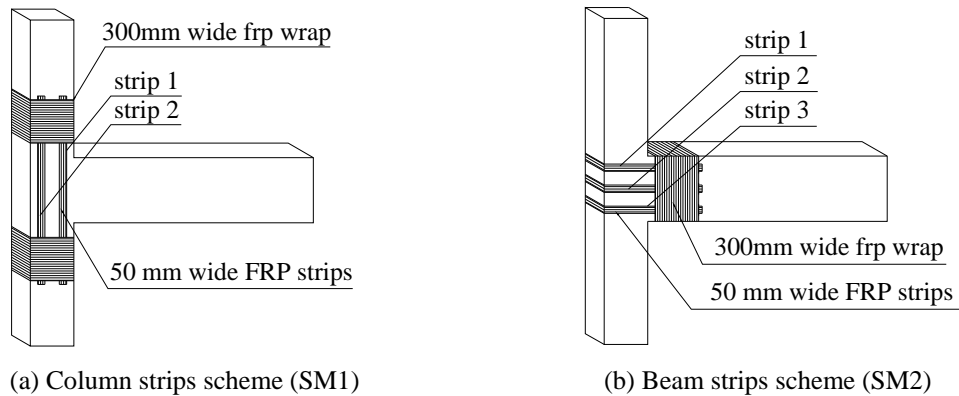


Fig. 3 FRP strengthening scheme and summary of FRP strain gauges

All the connections were void of transverse reinforcement in the joint region and the geometric properties and reinforcement details are shown in Fig. 2. In addition, the flexural strength ratio of the column to the beam was 1.40. The connections were designed to fail in the joint region first for the control specimen as well as the FRP-strengthened specimens. Failure of the FRP was particularly important so that the strength and behaviour of the FRP strengthening could be captured. It should also be noted that the commonly recognised philosophy for designing seismically resistant RC frames is, however, based upon the strong column-weak beam principle in which the beam ultimately fails first.

Two different FRP strengthening techniques were considered in which two layers of carbon FRP (CFRP but herein referred to as FRP) strips formed from carbon fibre sheets in a wet lay-up process were applied to the joint region. The *column strip* scheme (Fig. 3(a): Specimen SM1) consisted of two 50 mm wide strips bonded either side of the joint face which extended into the column. Two layers of wraps were then provided on both ends of the strips on the column in order to provide anchorage against complete strip debonding. The *beam strip* scheme (Fig. 3(b): Specimen SM2) consisted of three FRP strips oriented parallel to the longitudinal axis of the beam. The free ends of the strips were anchored by wrapping two layers of fibre sheet around the beam.

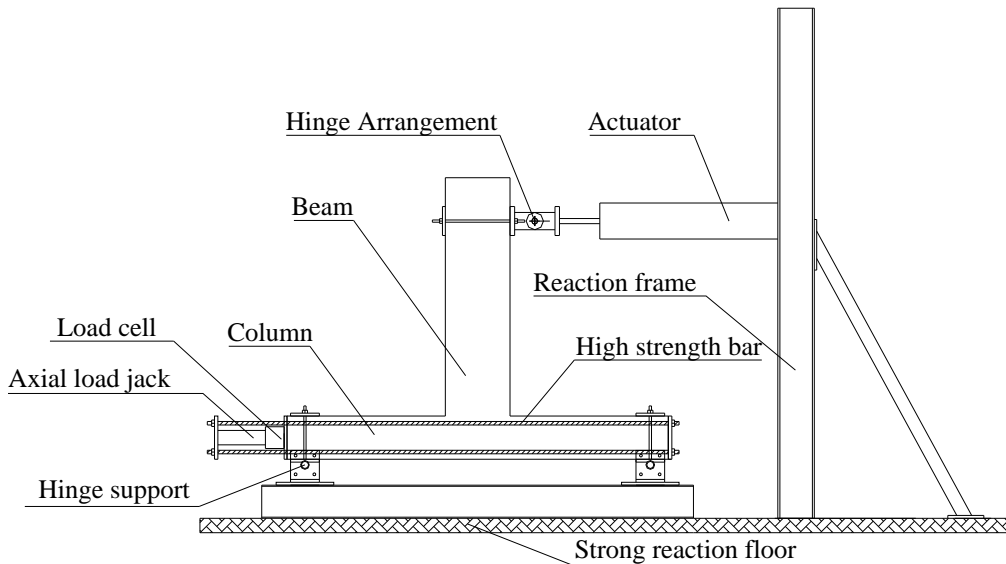


Fig. 4 Test setup

All FRP was applied in accordance with the manufacturers specifications and all concrete corners were rounded to a radius of 25 mm.

In reality, the RC beam-column connection shown in Fig. 3 may be cast with transverse beams originating from the joint region. In addition, there may also be a slab present. In order to strengthen such a complicated three-dimensional slab-connection, a possible strengthening scheme (although untested to date) may involve drilling vertical or horizontal slots through the transverse beams (and slab where appropriate) and epoxying FRP strips through such slots in order to strengthen the joint region in shear. The two-dimensional connection and FRP strip strengthening arrangements shown in Fig. 3 therefore can serve as a precursor to the three-dimensional connection strengthening scenario. The testing and modelling of three-dimensional connections is complicated, however, investigation of the two-dimensional connections shown in Fig. 3 serves as a good starting point.

The concrete properties on the day of the corresponding connection test are given as follows for specimens UM1, SM1 and SM2, namely (1) cylinder compressive strength = 25.4 MPa, 25.6 and 25.6 MPa, (2) modulus of elasticity = 24.18, 24.08 and 24.24 GPa, (3) splitting tensile strength = 2.82, 2.51 and 2.67 MPa and (4) modulus of rupture = 4.38, 5.31 and 4.54 MPa. The yield stresses of the longitudinal, and transverse steel reinforcing bars were 532 MPa and 332 MPa, respectively. The modulus of elasticity, tensile strength and ultimate strain of the FRP (nominal carbon fibre sheet thickness of 0.117 mm) were 243 GPa, 3,120 MPa and 1.1%, respectively.

The test set-up is shown in Fig. 4. The connection was mounted on a stiff test rig with hinge supports at both ends of the column and an axial load of 180 kN was applied to the column via a self-reacting frame. All three connections were tested under monotonically increasing load in deflection control of 10 kN increments at a loading rate of 0.2 mm per second. All test connections were extensively instrumented. Twelve variable displacement transducers (LVDTs) were utilised; three to measure deflection along the length of the beam while the remainder were used for monitoring reaction frame movements. The internal steel reinforcement was extensively

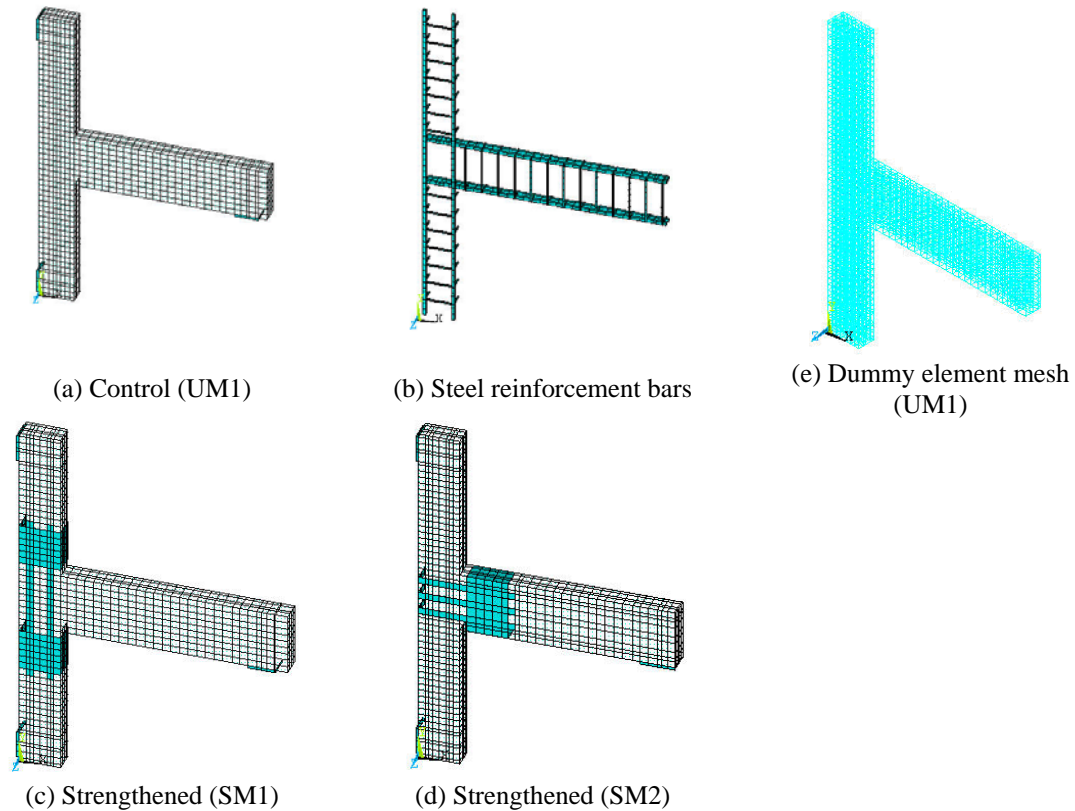


Fig. 5 Finite element meshes

instrumented with 5 mm gauge length strain gauges. Additional gauges of 5 mm gauge length were also adhered onto the FRP surfaces for the FRP-strengthened connections. Seven strain gauges were attached on each FRP strip on the front face and three gauges each on the back face for the connection with column strips and nine gauges on each FRP strip (five on the front, two on the back and two on the side face) for the connection with beam strips. The exact positions of these gauges are not shown in this paper, however, full details can be found in Shrestha (2009).

### 3. Finite element modelling details

A comprehensive description of the FE modelling procedure is given in this section. Additional comments of a more generic nature are also given in order to provide a deeper understanding of the FE modelling of FRP-strengthened RC connections with ANSYS.

#### 3.1 Mesh

The concrete element used in the mesh is only available in a three-dimensional format, hence the need to model three-dimensionally. Coupled with the desire to discretely model the steel reinforcement bars and the wrapping of the FRP around the column (Fig. 3(b)), a three-

dimensional FE model was also constructed. A mesh sensitivity analysis was carried out for the plain connection and an optimum mesh size based on a convergence of the beam-tip elastic deflection was selected. This mesh was then used for modelling both the plain and FRP strengthened connections. Only half of the width (i.e., out of page or z-direction) of the connection was modelled by taking advantage of symmetry. The size of the mesh was also governed by the location of the steel reinforcement bars. The finite element models with the optimum mesh sizes for connections UM1, SM1 and SM2 are shown in Fig. 5. A fine mesh was used in the joint region while a relatively coarse mesh was used in the beam and the column. The element sizes varied from 25 mm to 90 mm in the X-direction, 25 mm to 50 mm in the Y-direction and 34 mm to 52 mm in the Z-direction. The models were four elements thick in the Z-direction in order to include the concrete cover. The total number of elements used for the concrete, steel supporting plates and steel reinforcing bars were 2768, 52 and 579, respectively, and for the FRP the total number of elements used were 292 for SM1 and 142 for SM2. The ends of the column were pin supported and the load was applied by increasing the beam-tip displacements.

### *3.2 Elements*

Concrete was modelled using the SOLID65 element, which is an eight-node solid element capable of simulating plastic deformation, crushing and cracking in orthogonal directions, with the cracks modelled as smeared bands. Smeared cracking is acceptable in this FE study as it is the overall load-deflection behaviour that is of primary concern. To represent the condition at the crack face, shear transfer coefficients of 0.3 for open cracks and 0.7 for closed cracks were adopted in this study, from trial and error, as these values were found to produce the most stable models. Choosing lower values led to convergence difficulties whereas higher values resulted in stiffer models.

Internal steel reinforcement bars were modelled with two-node three-dimensional LINK8 spar elements. The stress in each steel element, however, does not vary due to the smeared crack approach taken by the concrete element. The FE strains in the steel reinforcement are therefore expected to be higher than that observed in reality due to the inability of a smeared crack approach to model tension stiffening.

The FRP strengthening was modelled with four-node three-dimensional SHELL181 elements having in-plane stiffness but no bending stiffness. Other ANSYS models that have been developed for FRP-strengthened connections (i.e., Parvin and Granata 2000, Mostofinejad and Talaeitaba 2006) used three-dimensional SOLID45 elements to represent the FRP. The main disadvantage of this element is the thickness of the element having to be defined which can lead to distorted aspect ratios considering the FRP is so thin compared to its surface area.

The SOLID45 element was used to model the steel supporting plates at the end of each column and the point of load application at the free-end of the beam.

To model the slip between the concrete and steel reinforcement bars, an interface element was introduced between the concrete and steel reinforcement bar element nodes. The unidirectional COMBIN39 element was used for this purpose and programmed to simulate the fib (2000) relationship describing slip between internal steel reinforcing bars and surrounding concrete.

### *3.3 Dummy elements and tension stiffening*

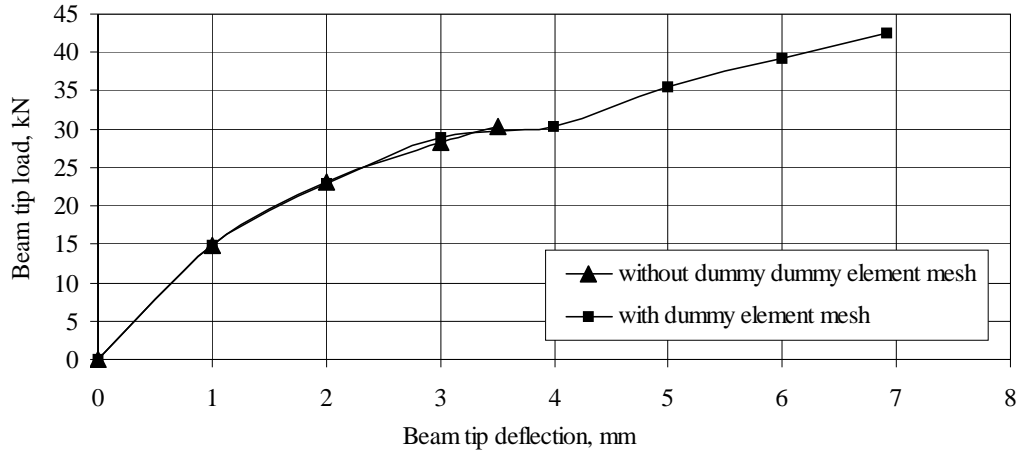


Fig. 6 Load-deflection plots for a connection with and without dummy element

Instability of the reference connection FE model occurred when the elastic modulus of the concrete was set to zero by ANSYS immediately after cracking. Non-convergence resulted due to excessively large displacements of cracked element nodes. To overcome this problem, two-node three-dimensional LINK8 spar dummy elements of  $1 \text{ mm}^2$  cross-sectional area with the same properties as that of concrete and were added to the model. The dummy elements were then distributed throughout the joint, beam and column in three orthogonal directions. Dummy elements were not required for the FRP-strengthened connections as the FRP layer of elements held cracked elements in place. Also, dummy elements did not appreciably alter the stiffness of the connection as seen in Fig. 6.

Tension stiffening has not been explicitly modelled herein owing to the use of a smeared crack approach. The dummy elements however, especially in the concrete tension region, can be used to simulate tensile force carried by the concrete between cracks although such a course of action has not been utilised in this study and is therefore left for future research. Another way that tension stiffening has been treated in the past by other researchers has been by increasing the stiffness of the steel reinforcement (Gilbert and Warner 1977). Dummy elements will still, however, need to be used in the FE model in order to prevent non-convergence at low loads due to cracking in the concrete cover.

### 3.4 Constitutive relationship of concrete and concrete element crushing capability

The stress-strain relationship of concrete is modelled using Desayi and Krishnan's (1964) model. Softening of the concrete beyond the peak stress has been ignored and perfectly plastic behaviour assumed because inclusion of the softening component caused non-convergence. Linear elastic behaviour of concrete is considered up to the first point in the plot which corresponds to 30% of the maximum compressive strength. The ultimate strain is 0.003 (AS 3600 2001) and Poisson's ratio for concrete has been taken as 0.2 as per the AS3600-2001 recommendations.

When the concrete crushing capability was activated, it was found that the FE model for the reference connection failed prematurely, as was also found by Kachlakev *et al.* (2001). On account

of stress concentrations around corners, the concrete stresses were found to exceed the ultimate stress capacity this resulting in localised failure due to crushing of concrete at load levels much smaller than anticipated. Since failure by pure crushing of concrete was deemed unlikely, the crushing capability of the concrete elements was turned off in order to facilitate better model convergence.

### *3.5 Support condition and loading*

Steel plates were modelled at the support and load locations. Column ends were restrained at their ends to simulate hinge supports such that the effective length of the column between the supports was 2400 mm and the beam tip load was applied at a distance of 1625 mm from the column centre line. A load of 90 kN was applied to each end of the column in order to simulate the axial load of 180 kN applied in the test as only half of the connection was modelled. The beam end was subjected to increasing deflection to simulate the loading. Each load step consisted of increasing deflection by 1 mm.

### *3.6 Failure criterion and load steps*

In order to solve the non-linear governing equations, ANSYS utilizes the Newton-Raphson method (ANSYS 2007). A number of convergence-enhancement and recovery features, such as line search and automatic load stepping, were activated in order to help the model to converge.

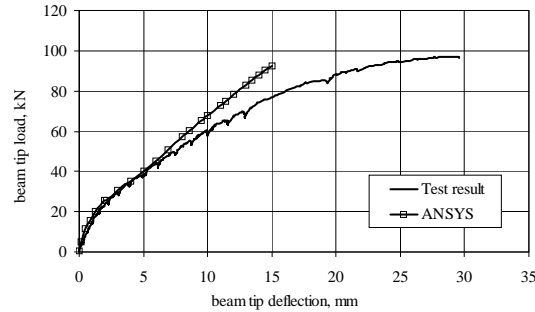
With the automatic time stepping option for non-linear analysis, the load sub-step sizes which governs the size of the load increment in subsequent steps are calculated based on the previous solution history of the model. The minimum and maximum load step sizes calculated by the automatic time stepping option are based on the input parameters of the model. Prior to cracking of the concrete, the maximum sub-steps chosen were 20 as the concrete would behave linearly in this range. In the post cracking stage, however, the maximum sub-steps were increased to 1000.

In some nonlinear static analyses, using the Newton-Raphson method alone may cause the tangent stiffness matrix to become singular (or non-unique), thus causing severe convergence difficulties. Such occurrences include nonlinear buckling analyses in which the structure either collapses completely or "snaps through" to another stable configuration (ANSYS 2007). For such situations, an alternative iteration scheme, the arc-length method, can be activated to help avoid bifurcation points and track unloading. The arc-length method has, however, not been used in this study.

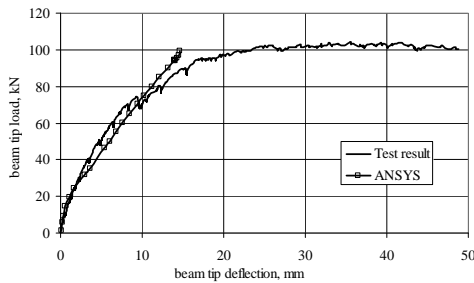
## **4. Analysis of results: simulation and test**

### *4.1 Beam-tip load-displacement response*

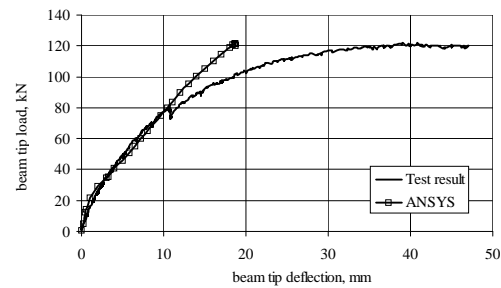
The load versus displacement responses for all three test connections is shown in Fig. 7. The peak load is accurately predicted by the FE models, however, the beam-tip deflection in the overload region is poorly modelled. The solution stopped when one or more concrete nodes suffered large displacement as a result of excessive cracking and the compressive strength of concrete being exceeded. Despite the modelling of slip of the internal steel reinforcing bars, the deflection is still underestimated by generally more than 50%. Several explanations can be offered



(a) Control specimen UM1



(b) FRP-strengthened Specimen SM1



(c) FRP-strengthened Specimen SM2

Fig. 7 Load versus displacement responses

for his discrepancy, namely (1) the inability of the model to simulate debonding of debonded FRP in the joint region may result in an overestimation of the joint stiffness, (2) inability to adequately capture joint shear distortion, and (3) possible support movements in the experimental work not being considered in the FE model (for instance, linear-elastic analysis reveals a support movement of 1 mm to cause a beam tip deflection of 1.46 mm). It is clear that the beam-tip movement is magnified with support movement. As possible support movements were not measured in the tests of Shrestha (2009), the amount of actual beam-tip displacement due to support movement is thus speculative. Therefore, the remainder of results are concerned with load, and not displacement, and hence they can be viewed with confidence. On the subject of load though, it can be observed that the column oriented FRP strips in Specimen SM1 (Fig. 7(b)) are proven by test and numerical simulation to be largely ineffective as the peak load is only slightly higher than that of the control specimen UM1 (Fig. 7(a)). In addition, the FE model was not able to capture the peak load plateau arising from flexure failure especially evident in Figs. 7(b) and (c) due to loss of model stability.

## 4.2 Cracking behaviour and failure modes

### 4.2.1 Control connection UM1

Based upon experimental observations during connection loading, minor flexural cracks in the beam and cracks at the beam-column corner were followed by cracking in the joint region. Severe diagonal shear cracks were observed in the joint region at a load of 70 kN (13.2 mm beam tip deflection but herein referred to as deflection). A peak load of 96.4 kN (27.7 mm deflection) was

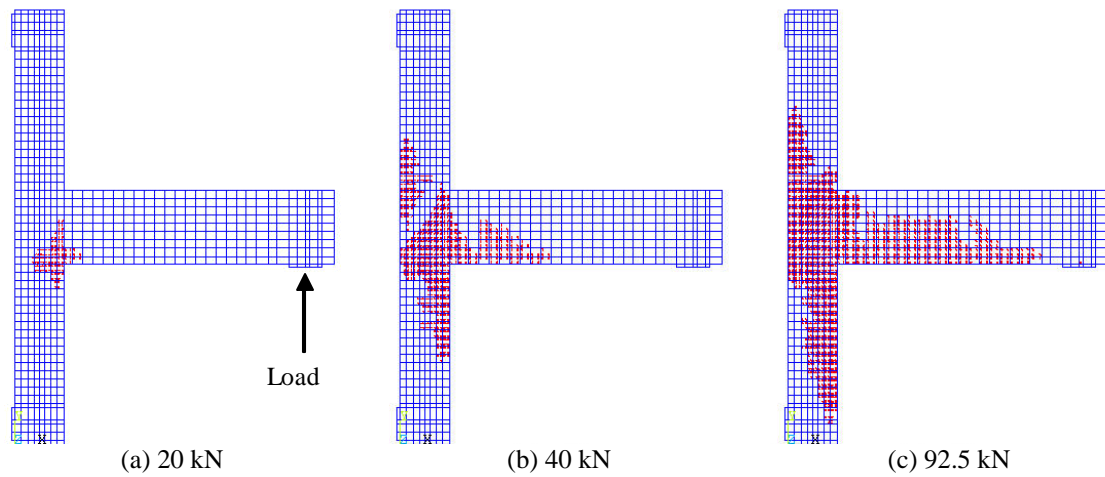


Fig. 8 Progression of cracking in control specimen (UM1)

observed following which the connection lost its load carrying capacity owing to severe shear cracking in the joint region.

The numerical simulation of the progression of cracking is shown in Fig. 8. Diagonal shear cracks originating from the beam-column corner and flexural cracks in the beam can be seen to develop at a load of 20 kN (Fig. 8(a)) and similar to test observations. With increasing load, the shear cracks extended into the joint region while flexural cracks extended into beam and column. Clear indications of diagonal shear cracks in the joint region are evident at loads of 30 kN and 40 kN (Fig. 8(b)). The severity of the cracks increased at higher load levels while the cracks also extend in the beam and the column (Fig. 8(c)). The test was stopped shortly after the peak load was reached and the final crack patterns are shown in Figs. 9(a) (test) and 9(b) (simulation) (note that the orientation of the finite element model has been changed for ease of comparison with the tested connection orientation). Although no detailed information can be extracted from the crack patterns, they nonetheless are affected especially by the beam oriented strips. The average shear crack was measured at 34 degrees to the horizontal (column) axis from tests although such an angle was unable to be extracted from the simulation. The finite element model is, however, able to capture the critical shear cracks in the joint region of the connection accurately and hence is able to predict the joint shear failure mode of the connection.

#### 4.2.2 FRP Column strip-strengthened connection SM1

Some minor flexural cracks were observed in the test specimen in the beam as it was loaded up to 10 kN. Cracks developed at the beam-column corner at a load of 20 kN (2 mm deflection) which propagated towards the joint centre with increasing load until it intersected the FRP and then propagated along the direction of FRP. A diagonal crack was observed in the joint region as the load was increased from 70 kN to 80 kN (19 mm deflection) with simultaneous cracking heard indicating localised debonding of the FRP. The last crack marking was carried out at a load of 90 kN following which the specimen was loaded continuously. The peak load of 103 kN was achieved at a deflection of 32 mm when FRP strip 1 debonded along its whole length followed by a loss of load carrying capacity of the connection. The primary mode of failure was debonding of the FRP strips in the joint region followed by joint shear failure. Concrete spalling was also

observed at the beam-column corner on the compression face of the column. The column wraps which secured the ends of the FRP strips prevented the strips from completely debonding, however, the column wraps were not effective in preventing localised debonding in the joint region. No rupture of the FRP was observed and the FRP provided little restraint to the opening of critical

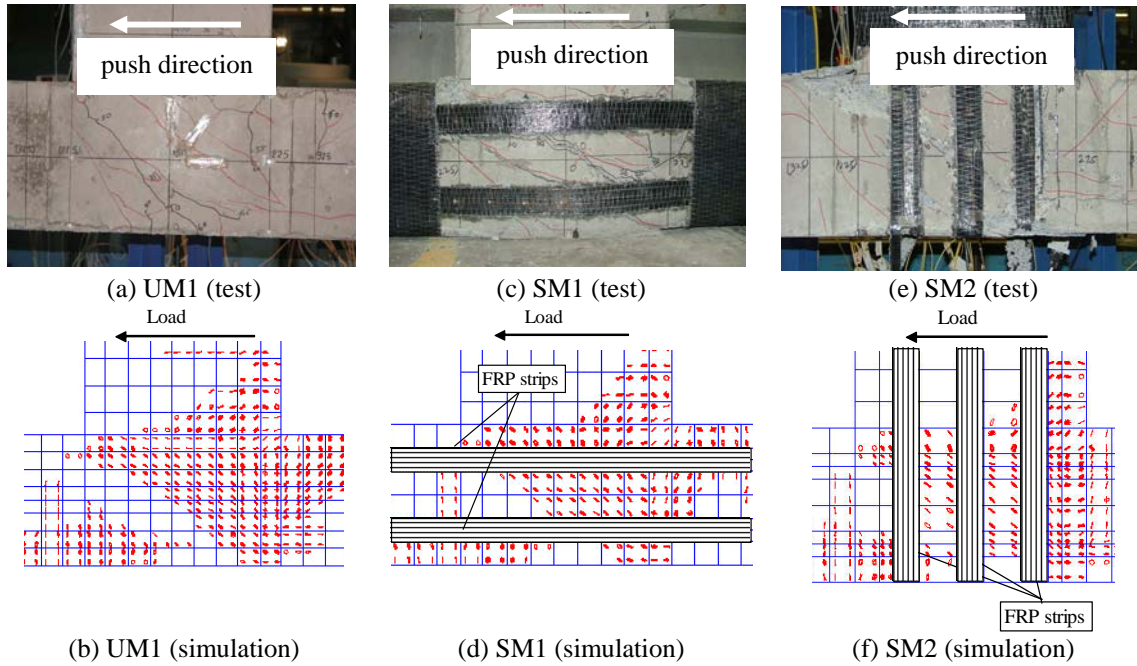


Fig. 9. Final crack patterns for tested and simulated specimens

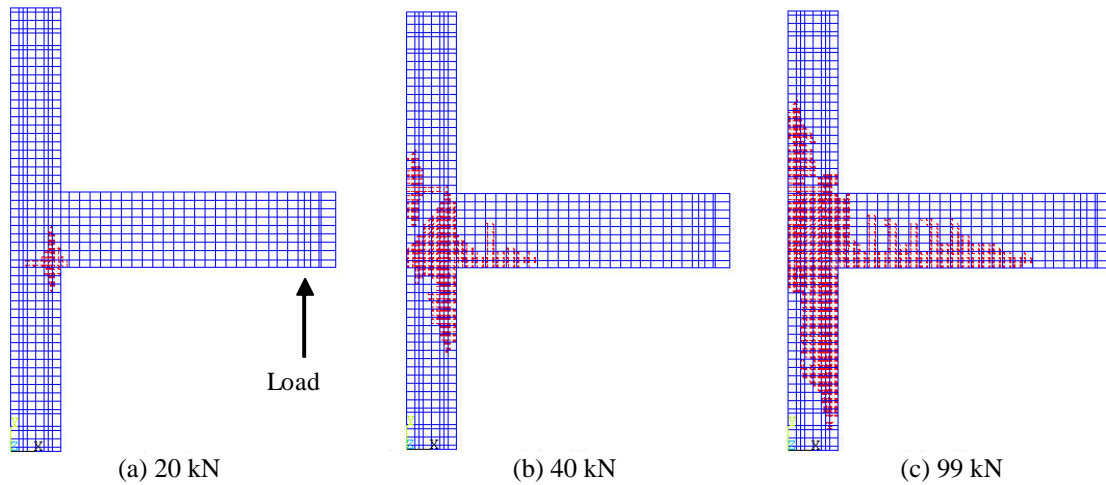


Fig. 10 Progression of cracking for column strip scheme (SM1)

shear cracks in the joint region.

The simulated progression of cracking is shown in Fig. 10. Shear cracks started to appear at the corner where the beam meets the column at 20 kN load (Fig. 10(a)). With increasing load, cracks extended into the joint region while flexural cracks in the beam and column were observed and the severity of these cracks intensified (Figs. 10(b) and (c)). Comparison of joint crack patterns with the control connection, UM1 (Figs. 8(b) and (d)), shows the reduced extent of cracks at identical load levels in connection SM1. The crack pattern from the finite element model is compared with test observation in Figs. 8(c) and (d). It can be seen that the FE model is able to capture the critical shear cracks in the joint region of the connection. The final crack pattern in the joint region is shown in Fig. 7(b) and the average test shear crack angle was measured at 37 degrees to the column axis. The crack angle has been influenced by the presence of the FRP.

#### 4.2.3 FRP beam strip-strengthened connection SM2

The experiment revealed a fine crack at the beam column corner at 10 kN load which propagated horizontally towards the beam centre and crossed the FRP strips with increasing load, while flexural cracks were observed in the beam. Unlike connection SM1, severe diagonal cracking in the joint region was not observed until the load reached 80 kN (11.5 mm deflection). This was attributed to the confinement provided by the FRP strengthening where the FRP strips which were wrapped around the column and anchored by the FRP wrap provided some resistance to joint shear distortion. At 80 kN load (11.5 mm deflection), local debonding of strip 3 was observed and the load dropped. The last crack marking was carried out at 90 kN load (14.7 mm deflection) where diagonal shear cracking was observed to form in the joint region, following which the connection was loaded continuously. A peak load of 122 kN was achieved at a deflection of 39.1 mm when FRP strip number 3 debonded. This was followed by debonding of FRP strips 2 and 1. The connection lost its load carrying capacity considerably as a result of shear failure which was followed by debonding along the length of all three FRP strips. Spalling of concrete at the beam-column corner on the compression face was also observed. Sequential rupture of FRP strips 3, 2 and 1 occurred as the loading was continued at load/deflection of 98 kN/67 mm, 81 kN/81.5 mm and 62 kN/92 mm, respectively.

The simulation revealed cracking at increasing beam tip loads as shown in Fig. 11. Unlike the experiments, the FE model simulated cracking from virtually the outset of the analysis and just like the other test specimens although the extent of cracking at 20 kN was much less than the amount of cracking at the same load level in specimens UM1 (Fig. 8(a)) and SM1 (Fig. 10(a)). Such discrepancy between test and theory for SM2 is believed to be due to the confinement action of the FRP strips not being properly modelled. Ideally the stress-strain relationship of the concrete, at least in the joint region, should consider confinement effects. As the analysis proceeded, shear cracks extended into the joint region with increased load while flexural cracks appeared in the beam and the column. However, the extent of cracking was less severe when compared to connections UM1 and SM1 at identical load levels suggesting that the confinement effect of the FRP was indirectly considered in the model. Joint diagonal shear cracks formed and the severity of the cracks further increased and extended throughout the joint with further development of the flexural cracks in the column and the beam at higher load level until the peak load (Fig. 11(c)). The finite element model was able to capture the shear cracks in the joint region as shown in Figs. 9(e) and (f). The average shear crack angle was measured to be at 30 degrees to the column axis and the effect of the FRP on the shear crack angle is evident.

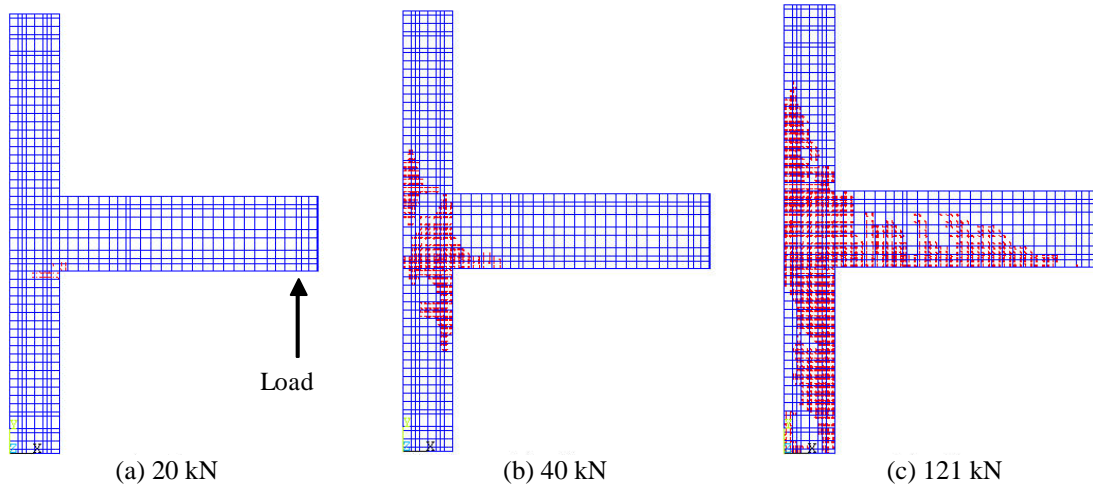


Fig. 11 Progression of cracking for beam strip scheme (SM2)

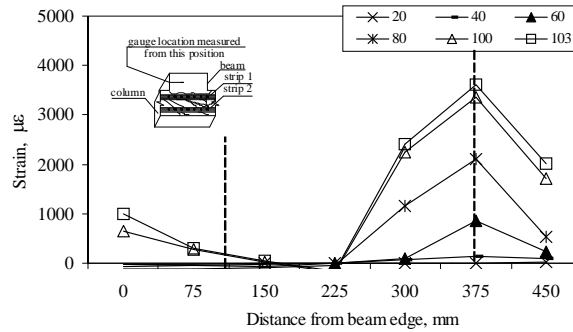
#### 4.3 FRP stress and strain distribution

One of the key features of this study was the determination of strain (and stress) distribution along the length of FRP strips in FRP-strengthened connections. The results of which are detailed as follows.

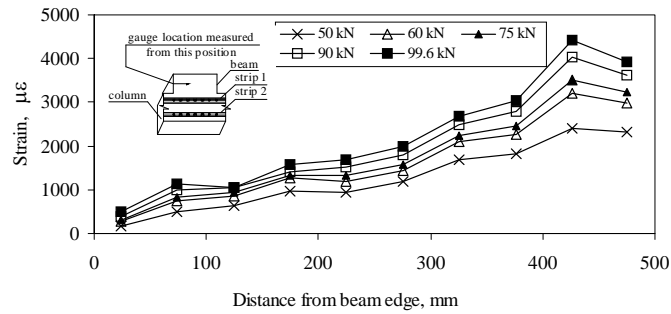
##### 4.3.1 FRP column strip-strengthened connection SM1

The strain profile along the length of the FRP strips 1 and 2 from the FE model is compared with the test results in Fig. 12. The test strains are based on the strain gauge readings at a particular location with vertical dashed lines representing the position of shear cracks intersecting the FRP. It should be noted though that the strain gauges were not located exactly where the shear cracks intersected the FRP strips (as the location of the cracks could not be pre-determined) and hence the recorded strains may only represent strain close to the peak strain values. The position of the simulated strain results are shown at different positions along the length of the FRP on account of the mesh geometry being independent to the strain gauge positions. Similar to the results from the test, strip 1 was found to attract more strain. In addition, similarities in the distribution of the strain along the lengths of the FRP strips between simulation and test can also be seen in Fig. 12 with the maximum strains being quite similar. This similarity is despite the fact the strips debonded in the tests but were not modelled so in the analysis. Therefore, it can be concluded that the finite element model is effective in capturing the strain distribution along the length of the FRP strips and can be used to predict the critical location in FRP for debonding. In Fig. 12, which shows the strains corresponding to loads ranging from 20 kN to a maximum of 103 kN, high FRP strain can be observed in the region adjacent to shear cracks indicating debonding of FRP while low FRP strain regions are those where the bond between FRP and concrete was not lost and full interaction between the two was maintained.

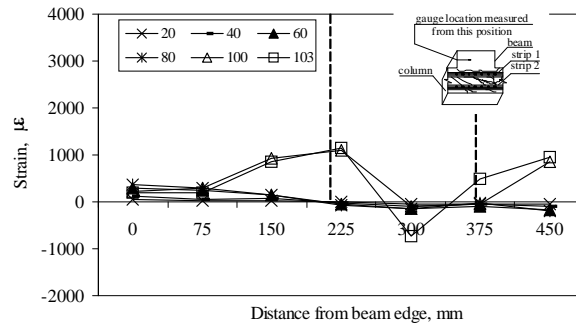
The simulated stress distribution (in MPa) in the FRP strips at different load levels are given in Figs. 13(a) and (b). Strip 1 is subjected to higher stresses than strip 2 with the difference in stress between the strips being consistent with test observations. Therefore, strip 1 is more susceptible to



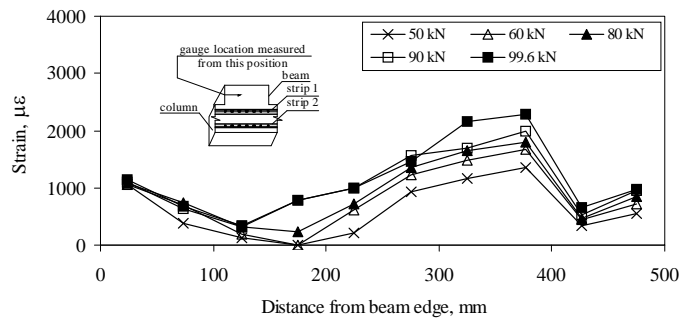
(a) Test (Strip 1)



(b) Simulation (Strip 1)



(c) Test (Strip 2)



(d) Simulation (Strip 2)

Fig. 12 Tested and simulated FRP strain distributions (SM1)

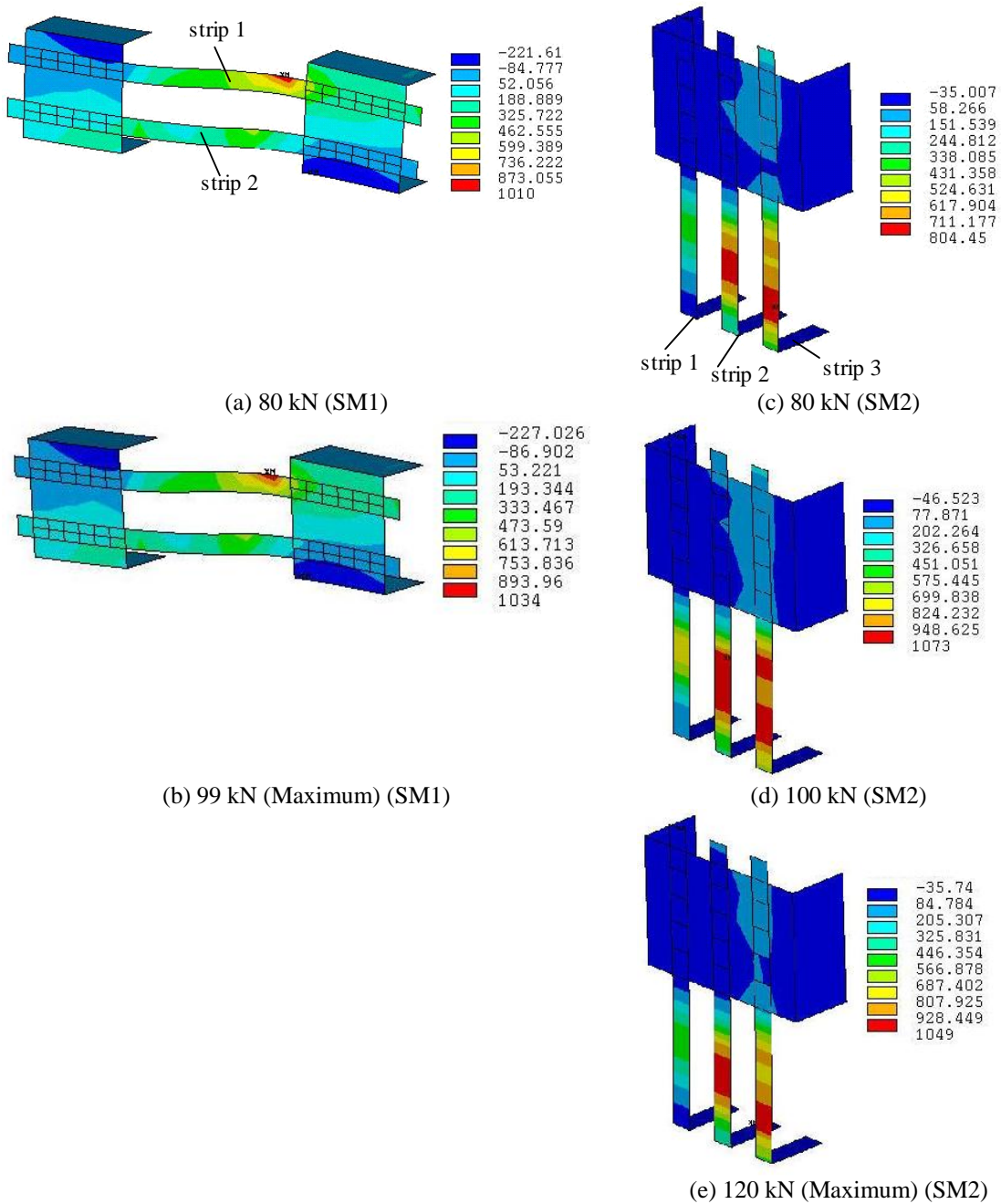


Fig. 13 Simulated FRP stress distributions (SM1 and SM2)

debonding. The maximum stress in strip 1 at the peak load was 1034 MPa which is close to the debonding stress value of 1094 MPa (calculated from Chen and Teng’s 2001 bond strength model).

4.3.2 FRP beam strip-strengthened connection SM2

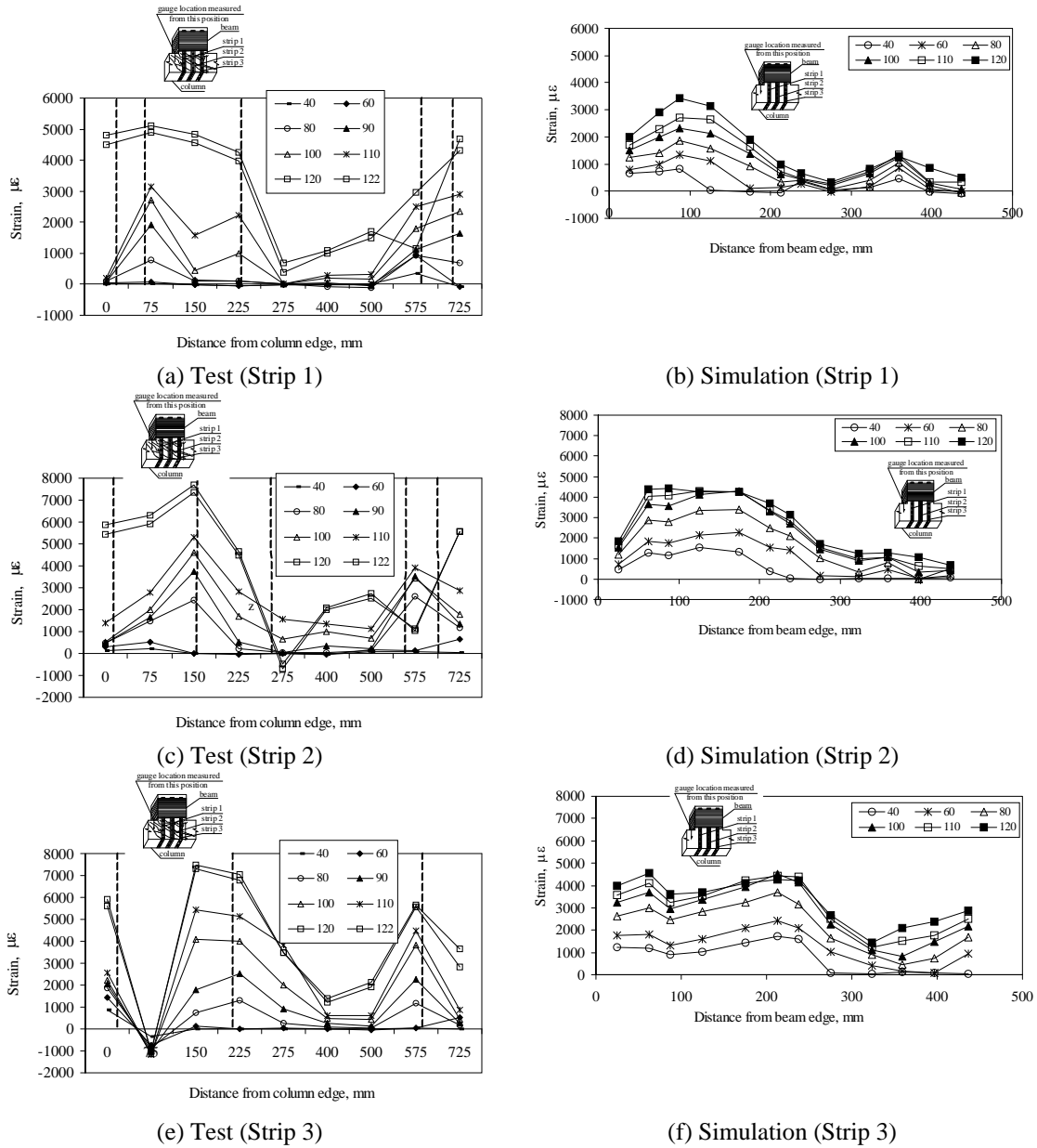


Fig. 14 Tested and simulated FRP strain distributions (SM2)

Fig. 14, shows the predicted and tested strain distribution along the three strips in connection SM2 with intersecting shear cracks indicated by vertical dashed lines. The finite element results were able to simulate the strain profiles along the length of the FRP strips reasonably well in the service load range. However, as the ultimate FRP stress and strain were limited to the debonding stress and strain based on Chen and Teng's (2001) model in the finite element model, the higher strain levels in the FRP strips observed in the tests beyond the FRP debonding and the peak load could not be replicated.

In Fig. 14 the strain results correspond to loads ranging from 40 kN to a maximum of 122 kN are shown. The reasonably uniform distribution of strain at high load in strip 1 of connection SM2 (Fig. 14(a) and to a limited degree in Fig. 14(b)) indicates the strip has debonded along a significant portion of its length. In addition, the higher level of strain in strips 2 and 3 are evident in Figs. 14(c)-(f), respectively. Also, even though the final mode of FRP failure was by rupture in connection SM2, the full rupture strain (1.1% obtained by coupon test) was never attained, primarily due to the bending of FRP strips around the edges of the joint region. Such a phenomenon has been observed in FRP shear-strengthened beams (Chen and Teng 2003) and confined prismatic columns (Wang and Wu 2008), for example, in which the FRP has been wrapped around a bend or corner.

Figs. 13(c) to (e) show the stress distribution in the FRP strips of the finite element model for connection SM2 at increasing load levels. Strips 2 and 3 are subjected to higher stress levels compared to strip 1 with similar difference in stresses in the three strips being observed in the test. The stresses in Strips 2 and 3 at the peak load are found to be 1074 MPa which is very close to the debonding stress value of 1096 MPa for the FRP strips based on theory (Chen and Teng 2001) and hence it can be concluded that debonding failure would be critical for the FRP strips.

The finite element model was able to accurately predict the stress and strain profiles along the FRP strip and hence provide vital information regarding critical regions in the FRP. Such information is of most importance as it will enable the designer to consider installing additional mechanical anchorage at high stress regions in order to prevent the propagation of debonding cracks on the length of the member. The prevention of the debonding will enable the connection to be designed to resist a higher load.

## **5. Conclusions**

This study has reported the strengths and limitations of modelling FRP-strengthened connections with ANSYS. The simulations have been compared with carefully documented and extensively instrumented tests. The numerical models were able to accurately predict the peak loads, crack patterns and stress distributions in the FRP and were able to identify critical (high stress) regions in the FRP strengthening. However, the results showed that the deflection at the peak loads could not be accurately predicted by the finite element models. While not explicitly modelling debonding between the FRP strengthening and concrete substrate, regions most susceptible to debonding (on account of high stresses) were, however, able to be isolated and such information is of most interest when designing additional anchorage along the length of the FRP strengthening for the prevention or delaying of debonding.

Experimental testing and numerical simulation has revealed the beam strips strengthening scheme (specimen SM2) to be more effective than the column strips strengthening scheme (specimen SM1). This is not only because the two FRP strengthening schemes were designed with different amounts of FRP (but with same FRP area to cross-sectional area ratio) but also because the beam strips scheme provided more confinement in the joint region and restraint against joint rotation. Rupture of FRP on connection SM2, unlike in the case of connection SM1, signifies a more effective use of strength of the FRP strips.

## **Acknowledgements**

This project was funded by Australian Research Council (ARC) Discovery Grant DP0559567. The financial assistance of the ARC is gratefully acknowledged.

## References

- ACI (2007), *Report on fiber-reinforced polymer (FRP) reinforcement for concrete structures*, ACI 440R-07, American Concrete Institute (ACI) Committee 440, Michigan, U.S.A.
- ANSYS (2007), *Release 11.0 documentation for ANSYS*, ANSYS Inc., USA.
- Antonopoulos, C.P. and Triantafillou, C. (2003), "Experimental investigation of FRP-strengthened RC beam-column joints", *J. Compos. Constr.-ASCE*, **7**(1), 39-49.
- AS3600 (2001), *Concrete structures*, Standards Australia, Homebush, Australia.
- Chen, J.F. and Teng, J.G. (2001), "Anchorage strength models for FRP and steel plates bonded to concrete", *J. Struct. Eng.-ASCE*, **125**(7), 784-791.
- Chen, J.F. and Teng, J.G. (2003), "Shear capacity of FRP-strengthened RC beams: FRP rupture", *J. Struct. Eng.*, **129**(5), 615-625.
- Desayi, P. and Krishnan, S. (1964), "Equation for the stress-strain curve of concrete", *ACI J.*, **61**(3), 345-350.
- El-Amoury, T. and Ghobarah, A. (2002), "Seismic rehabilitation of beam-column joint using GFRP sheets", *Eng. Struct.*, **24**(11), 1397-1407.
- Engindeniz, M., Kahn, L.F. and Zureick, A.H. (2005), "Repair and strengthening of reinforced concrete beam-column joints: state of the art", *ACI Struct. J.*, **102**(2), 1-14.
- FIB (2000), *Bond of reinforcement in concrete*, Bulletin 10, International Federation for Structural Concrete (fib), Luasanne, Switzerland.
- Gilbert, R.I. and Warner, R.F. (1977), *Nonlinear analysis of reinforced concrete slabs with tension stiffening*, UNICIV Report No. R-167, School of Civil Engineering, The University of New South Wales, Sydney, Australia.
- Granata, P.J. and Parvin, A. (2001), "An experimental study on Kevlar strengthening of beam-column connections", *Compos. Part B-Eng.*, **53**(2), 163-171.
- Hollaway, L.C. and Teng, J.G. (2008), *Strengthening and rehabilitation of civil infrastructures using fibre-reinforced polymer (FRP) composites*, Woodhead Publishing Limited, Cambridge, UK.
- Kachlakev, D., Miller, T., Yim, S. and Potisuk, T. (2001), *Finite element modelling of reinforced concrete structures strengthened with FRP laminates*, Oregon Department of Transportation Research Group, Salem and Federal Highway Administration, Washington, USA.
- Mahini, S.S. and Ronagh, H.R. (2011a), "Web-bonded FRPs for relocation of plastic hinges away from the column face in exterior RC joints", *Compos. Struct.*, **93**(10), 2460-2472.
- Mahini, S.S. and Ronagh, H.R. (2011b), "Numerical modelling for monitoring the hysteretic behaviour of CFRP-retrofitted RC exterior beam-column joints", *Struct. Eng. Mech.*, **38**(1), 27-37.
- Mostofinejad, D. and Taleitaba, S.B. (2006), "Finite element modelling of RC connections strengthened with FRP laminates", *Iran. J. Sci. Tech. Trans. B Eng.*, **30**(B1), 21-30.
- Parvin, A. and Granata, P. (2000), "Investigation on the effects of fiber composites at concrete joints", *Compos. Part B-Eng.*, **31**(6-7), 499-509.
- Parvin, A. and Wu, S. (2004), "Evaluation of wrap thickness on CFRP-strengthened concrete T-joints", *Proceedings, Second International Conference on FRP Composites in Civil Engineering, CICE 2004*, Adelaide, Australia, 643-646.
- Shrestha, R. (2009), *Behaviour of RC beam-column connections retrofitted with FRP strips*, School and Civil and Environmental Engineering, Faculty and Engineering and Information Technology, University of Technology Sydney, Australia.
- Shrestha, R., Smith, S.T. and Samali, B. (2009), "Strengthening of RC beam-column connections with FRP strips", *Proceedings of the Institution of Civil Engineers, Structures and Buildings*, Special Issue on Advanced Composites (Part II), **162**(SB5), 323-334.

- Shrestha, R., Smith, S.T. and Samali, B. (2011), "The effectiveness of FRP strips in repairing moderately and severely damaged RC beam-column connections", *Mag. Concrete Res.*, **63**(1), 1-16.
- Smith, S.T. and Shrestha, R. (2006), "A review of FRP-strengthened RC beam-column connections", *Proceedings, Third International Conference on FRP Composites in Civil Engineering, CICE 2006*, Miami, USA, 661-664.
- Teng, J.G., Chen, J.F., Smith, S.T. and Lam, L. (2003), "Behaviour and strength of FRP-strengthened RC structures: A state-of-the-art review", *Proc. Inst. Civil Eng. Struct. Build.*, **156**(1), 51-62.
- Wang, L.M. and Wu, Y.F. (2008), "Effect of corner radius on the performance of CFRP-confined square concrete columns: Test", *Eng. Struct.*, **30**(2), 493-505.

CC